ISSN 2063-5346

ANTIBACTERIAL AND ANTIFUNGAL PERFORMANCES OF PLATE –LIKE $MnAl_2O_4$ NANOPARTICLES PREPARED BY HYDROTHERMAL METHOD

R.V. Amudhini[1], P. Vasantharani[1*], G. Sivakumar[2]

Article History: Received: 11.02.2023 Revised: 07.03.2023 Accepted: 15.05.2023

Abstract

The hydrothermal technique was used to synthesize $MnAl_2O_4$ nanoparticles and the obtained nanoparticles were distinguished using numerous characterization facilities, such as X-ray Diffractometer, FE-SEM with EDS, FT-IR and HR-TEM. The individual crystalline size of $MnAl_2O_4$ nanoparticles was found to be 31 nm by the Debye Scherrer's method. FE-SEM was used to identify the morphology of the nanoparticles. Using a Fourier Transform Infrared Spectrometer (FT- IR), the functional group of $MnAl_2O_4$ nanoparticles was identified. Further, it was found that $MnAl_2O_4$ nanoparticles exhibited considerable antibacterial activity upon Gram-Negative (*Salmonella* sp and *E. coli*) and Gram-Positive bacteria (*Bacillus subtilis* and *Staphylococcus aureus*) respectively. It exhibited excellent antifungal properties against four pathogenic fungi, such as *Candida albicans*, *Candida tropicalis*, *Aspergillus niger* and *Mucorpiri formis,* respectively.

Keywords: $MnAl_2O_4$, Hydrothermal, Antibacterial, Antifungal, Crystalline size, Functional group.

[1]Department of Physics, Annamalai University.

[2]Centralised Instrumentation and Service Laboratory, Annamalai University, Annamalai Nagar, Chidambaram-608002, India

Authors for correspondence:selvamvasantharani@gmail.com

DOI: 10.48047/ecb/2023.12.5.275

1. INTRODUCTION

The unique crystal structure and morphological behaviour of spinel-structured metal oxide nanomaterial's have received a lot of attention in recent decades [1-5]. Semiconductors with a spinel structure are composed of a group of metal oxides with the chemical formula AB_2O_4, where A and B are divalent and trivalent cations, correspondingly. Semiconductor nanomaterials have been extensively investigated in the last few years both in the fields of nanoscience and nanotechnology due to their fundamental scientific interest and technological applications in interdisciplinary areas. Aluminates are now used as heterogeneous catalysts in various catalytic reactions due to their stability and reactivity [6]. Furthermore, a heterogeneous catalysts like spinel aluminates MAl_2O_4 (M = Mn [7], Zn[8], Co[9]) are non-toxic, eco-friendly and has excellent catalytic performance. It is low-cost, reusable catalyst with excellent mechanical, chemical and thermal stability [10]. Because of its potential applications in photocatalysis, sensors, wastewater treatment, catalysis and rechargeable batteries, $MnAl_2O_4$has received a lot of attention [11-12]. Antibacterial and antifungal applications of $MnAl_2O_4$ nano-particles have yet to beinvestigated, according to a review of the literature, and this study has focused on them. Co-precipitation [13], sol-gel [14], hydrothermal [15] and green synthesis [16] are various methods for producing $MnAl_2O_4$ nanoparticles. The hydrothermalmethod is one of the methods for the better crystalline phases of $MnAl_2O_4$n nanoparticles with good morphological behaviour.

This research aimed to look into the structural, morphological and functional group analysis of $MnAl_2O_4$nanoparticles using HR-TEM ("High-Resolution Transmission Electron Microscopy"), Powder XRD, FE-SEM("Field Emission Scanning Electron Microscopy"), FT-IR and to test antibacterial activity against Gram-ve (*E. coli and Salmonella sp*) and Gram+ve bacteria (*Staphylococcus aureus* and *Bacillus subtilis*) and antifungal activity against four pathogenic fungi namely *Candida albicans*, *Candida tropicalis*, *Aspergillus niger*,*Mucorpiri formis,* respectively.

2. MATERIALS AND METHODS

2.1.Choice of precursors

Aluminium nitrate nonahydrate $[Al(NO_3)_2{\cdot}9H_2O]$, manganese(II) acetate tetrahydrate $[Mn(CH_3COO)_2{\cdot}4H_2O]$ and sodium hydroxide [NaOH] were of AR grade and received with (99 percent)purity from Merck chemicals and utilized in the experiment without further purification.

2.2. Synthesis of $MnAl_2O_4$ nanoparticles by a hydrothermal method

Excellent purity Manganese acetate tetrahydrate $[Mn(CH_3COO)_2{\cdot}4H_2O]$ of 0.05 molarity and aluminum nitrate nonahydrate $[Al(NO_3)_2{\cdot}9H_2O]$ of 0.1 molarity were liquified in distilled water and stirred for 10 min to achieve a complete reaction between the two precursors. The pH level was then adjusted by adding suitable quantities of sodium hydroxide mixture dropwise into the obtained mixed solution. The suspension abruptly formed a brown solution. Further continuous stirring transformed the obtained solution to a dark brown, indicating $MnAl_2O_4$nanoparticles. The combined mixed solution was poured into an autoclave coated with Teflon for 24 h at 200°C to undergo the hydrothermal reaction in a hot air oven. The solution was dried for 2h at 100°C in a hot air oven after being repeatedly washed with distilled water and ethanol. The final product was calcined at 800°C for 5h in the Muffle Furnace for further characterization.

2.3. Characterization techniques

The crystalline nature of $MnAl_2O_4$nanoparticles was determined using XRD (X-ray Diffraction) utilizing the PW3040/60 X'Pert Pro PAnalytic Powder XRD with Cu Kα radiation (λ = 1.54060) at 40 kV and 30 mA. FE-SEM (ZEISS Supra 40VP) and the HR-TEM equipment were employed to analyze morphology. The particle size was determined with the FEI Tecnai G2 20 S-TWIN TEM. The FT-IR analysis was performed utilizing a Perkin Elmer by employing the KBr pellet technique in the 4000-400 cm^{-1}range to validate the functional groups.

2.4. Antibacterial activity

Petri plates were filled with Mueller-Hinton agar (MHA) medium. After the medium had been set, the inoculum was applied to the MHA plates using a sterile brush wetted with the bacterial suspension. Sterile samples were placed on the MHA plates together with 20µL of standard antibiotic (Ampicillin) discs. The samples were incubated on Petri plates at 37°C for 24h. To assess the antibacterial activity, the diameter of the inhibition zone was evaluated. The Agar Disc Diffusion technique was utilized to assess the sample's antibacterial activity.

2.5. Antifungal activity

The Disc Diffusion technique on SDA ("Sabouraud Dextrose Agar") medium was used to assess the extract's antifungal activity. The Petri plates were filled with agar medium. After the medium had hardened, the inoculum was applied to the solid plates using a sterile swab which was wet with the fungus suspension. As a positive control, amphotericin-B was used. The Petri plate samples were incubated at 37°C for 24h. This antifungal activity was then assessed by the inhibition zone diameter.

3. RESULTS AND DISCUSSION

3.1. Characterization

3.1.1. Phase analysis

XRD was utilized to determine the crystal structure as well as phase purity of the synthesized sample, as illustrated in Fig.1. 2θ values at 31.54°, 36.05°, 45.05°, 49.48°, 59.94° and 65.13° with hkl values of (220) (311) (400) (331) (511) and(440), confirmed that the synthesized $MnAl_2O_4$nanoparticles

were of the cubic phase with a spinel structure and Fd3m space group. The attained XRD peaks matched JCPDS card no 29-0880 [17]. The crystalline size was determined using the following Debye-Scherrerequation[18]:

$$D = \frac{K\lambda}{\beta\cos\theta} \quad (1)$$

Where crystalline size denoted D, the shape of the crystal denoted K (= 0.89), λ represented X-ray wavelength, β represented FWHM (Full Width at Half Maximum) and θ indicated Bragg's diffraction angle. Using the following formulae, the different factors, including Stacking Fault (SF), micro strain (ε) and dislocation density (δ) were determined from the XRD findings :

$$SF = \left(\frac{2\Pi^2}{45\tan\theta}\right)^{1/2} \quad (2)$$

$$\varepsilon = \frac{\beta\cos\theta}{4} \quad (3)$$

$$\delta = \frac{1}{D^2} \quad (4)$$

From the prominent peak(3 1 1), the crystalline size was determined to be 31 nm.

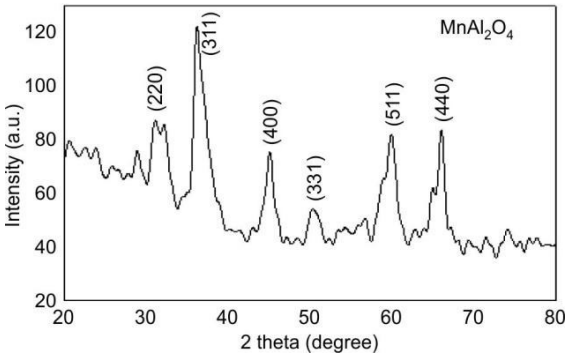

Fig 1. Phase analysis of $MnAl_2O_4$Nanoparticles (XRD)

The XRD analysis confirmed that the sample was free of impurities and ready for further characterization. XRD data were used to compute structural characteristics including the dislocation density, lattice parameter, microstrain, and stacking fault, as well as the crystalline size and it was found to be 0.57 lines/m, 8.03 Å, 3.69×10^{-3}, 6.11 and 31nm, respectively.

3.1.2. Functional group analysis

The $MnAl_2O_4$nanoparticles' functional groups were found using FT-IR spectroscopy. The spectrum of $MnAl_2O_4$Nanoparticles is shown in Figure 2. Adsorbed water stretching mode (O-H) was accountable for the peak at 3432cm^{-1}[19]. The less intense peak at 1647 $cm^{-1}$was corresponded to the bending vibration mode of the H-O-H group of the hydrated water. The peaks at 552 and 618 cm^{-1}were caused by the M-O Bond(Metal-Oxygen) of Al-O and Mn-O vibrational stretching modes and the development of the $MnAl_2O_4$spinel structure. All the findings were consistent with the previous reports[20,21].

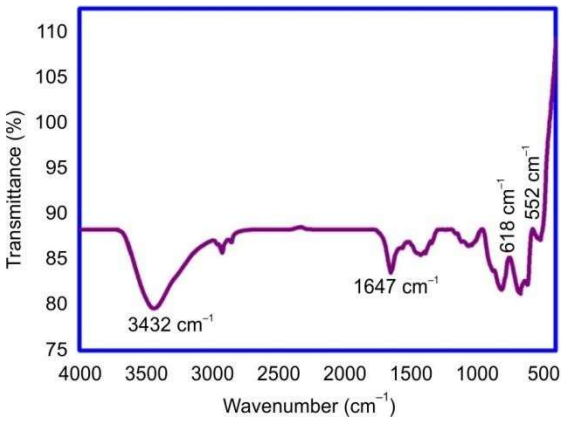

Fig 2. Functional group analysis of $MnAl_2O_4$nanoparticles(FTIR)

3.1.3. Morphology analysis

The morphology of $MnAl_2O_4$nanoparticles was studied using FE-SEM micrographs. Figure 3 shows FE-SEM pictures of $MnAl_2O_4$nanoparticles (f and g). The plate-like structure of the nanoparticles was visible. HR-TEM ("High-Resolution Transmission Electron Microscopy") pictures of $MnAl_2O_4$nanoparticles are shown in figures 3a, 3b, and 3c. The sample was regular cubic with a smooth surface, and the average particle size of MnAl2O4 nanoparticles from HR-TEM was calculated to be 35 nm (fig 3e).

The HR-TEM picture's measured interplanar distance (d = 0.24 nm) which exactly matched

the miller index (3 1 1) of the system that represented in the XRD pattern. The SAED pattern, as shown in Fig. 3d, confirmed the material's cubic structure and agreed well with the XRD data.The $MnAl_2O_4$nanoparticles HRTEM-EDAX spectrum was primarily composed of Mn, Al, and O elements, respectively [22].

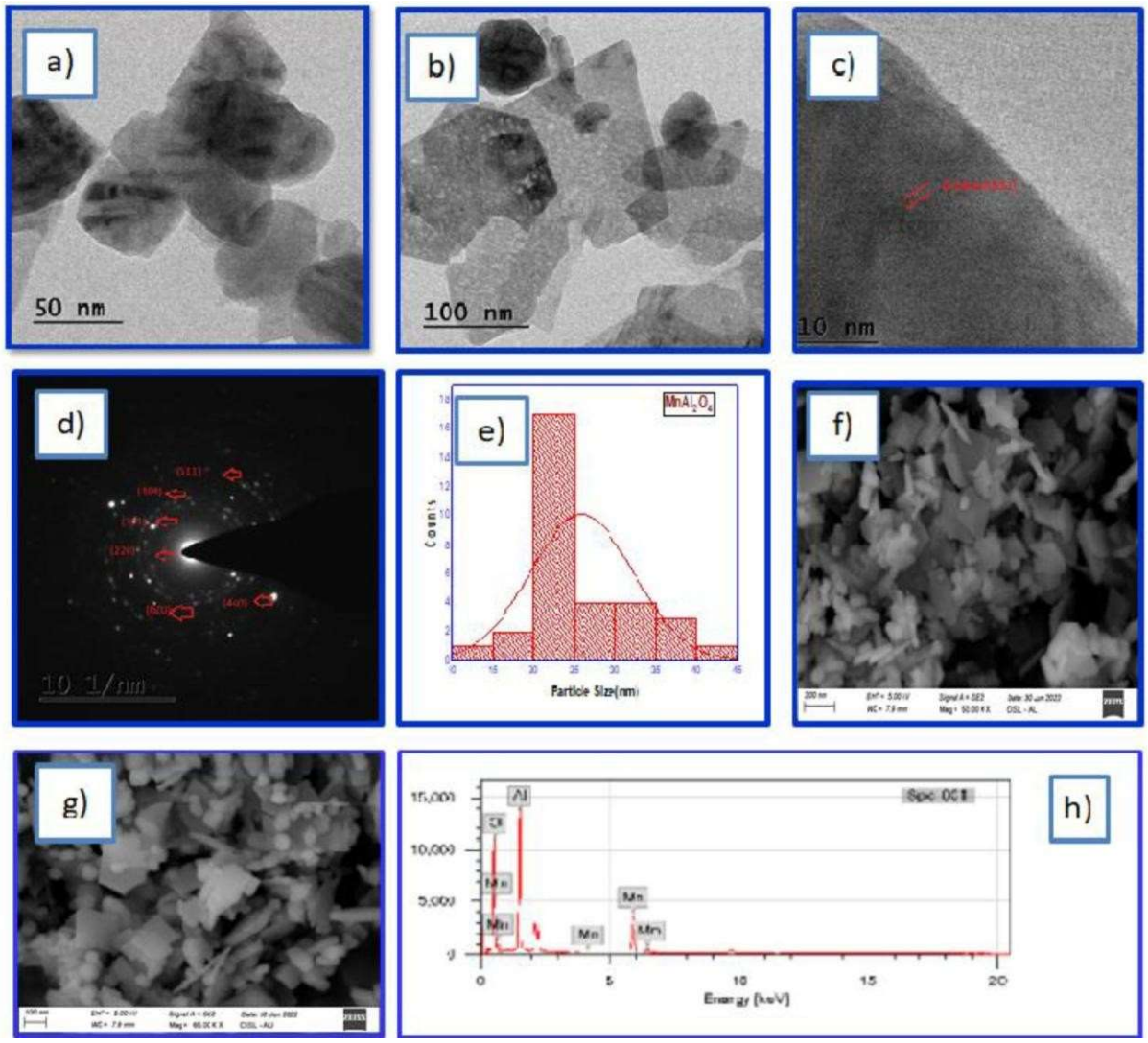

Fig.3.(a,b and c) HR-TEM images of $MnAl_2O_4$nanoparticles (d) SAED pattern (e)Particle size analysis of $MnAl_2O_4$nanoparticles (f,g) FE-SEM pictures (h) EDAX analysis of $MnAl_2O_4$nanoparticles.

3.2 Antibacterial applications

The Agar Disc Diffusion technique was used to assess the antibacterial effects of $MnAl_2O_4$Nanoparticles against Gram-Positive and Gram-Negative bacteriae including *S.aureus*, *B.subtilis*and *E.coli*, in addition to *Salmonella sp*pathogens, respectively (Fig 4). Table-3 displays the measured values for the zone of inhibition sizes. The antibacterial activities of each volume ratio of $MnAl_2O_4$nanoparticles were increased as the nanoparticle concentration increased. One possible mechanism involved in the antimicrobial application was the separation of the cell membrane due to the release of manganese and aluminum ions from $MnAl_2O_4$nanoparticles that bound to negatively charged bacterial cell walls and ruptured them, resulting in protein denaturation and cell death [23]. Metal oxides

actively inhibited bacterial growth by generating ROS (Reactive Oxygen Species), which could cause oxidative stress in bacterial cells [24].

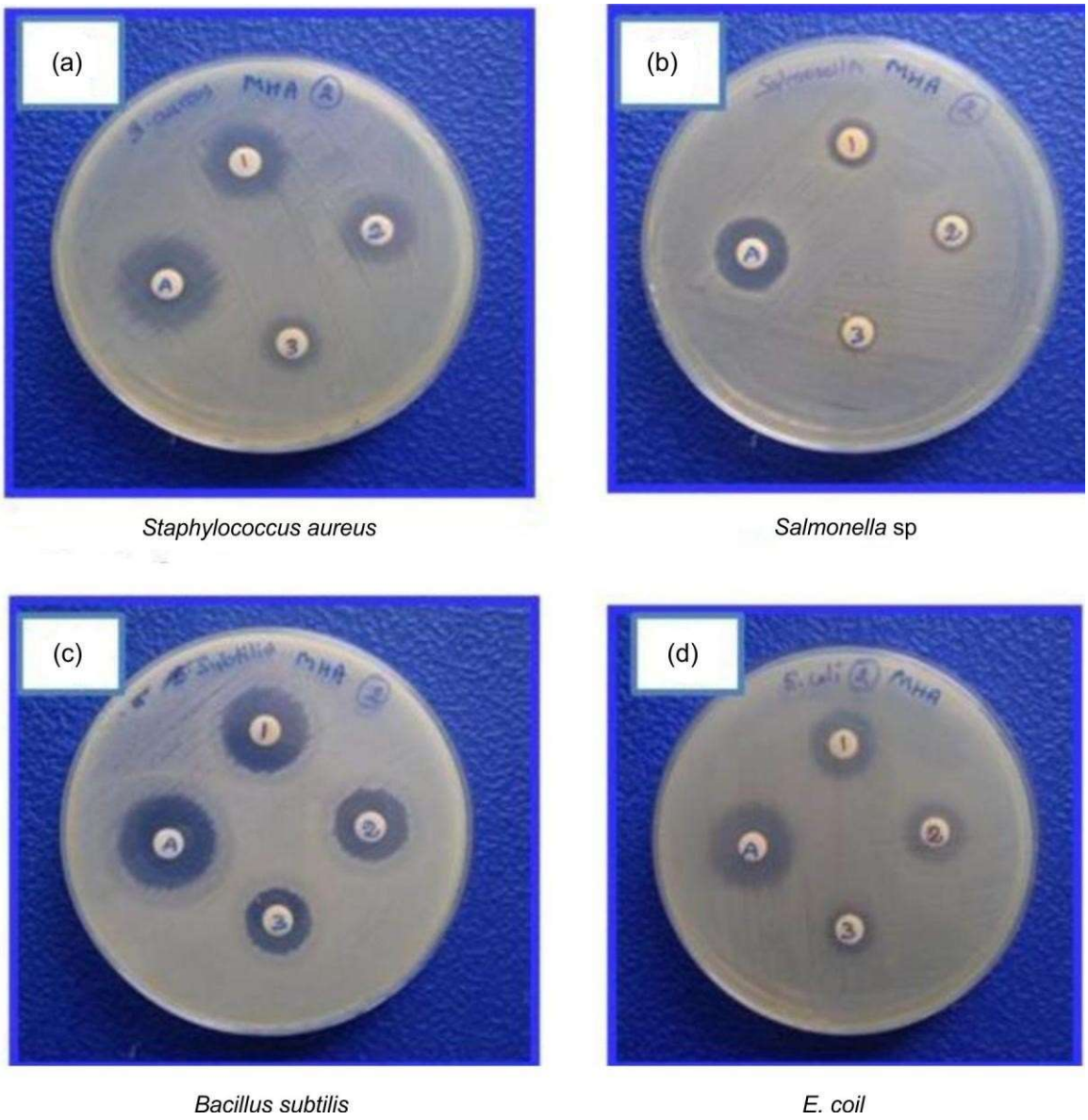

Fig 4. Antibacterial application of $MnAl_2O_4$nanoparticles against Gram +ve (a,c) and Gram -ve (b,d) bacteriae

Green synthesis was used by Shakeel Ahmad khan et al to synthesize MnO nanoparticles, which were then examined for their ability to inhibit the growth of Gram-Positive and Gram-Negative bacteria such as *B. subtilis, S. aureus, Bordetellabronchiseptica*and *E.coli* [25]. In contrast to Gram-Negative bacteria, MnAl2O4 nanoparticles demonstrated a maximal inhibition zone for Gram-Positive bacteria.

Table-1: Inhibition zone of $MnAl_2O_4$nanoparticles Zone of inhibition (mm)

Bacteriae	1000 (µg/mL)	Control
Staphylococcus aureus	6 mm	9 mm
E.coli	5 mm	9 mm
Bacillus subtilis	8mm	9 mm

Salmonella sp.	3 mm	6 mm

It might be excellently used for biomedical applications as it had the maximum capability rate for killing bacterial species in the cell wall. Among the bacteria selected, *Bacillus subtilis*had the highest sensitivity (8mm), followed by *Staphylococcus aureus*(6mm), *E.coli* (5mm) and *Salmonella* sp.had the lowest (3mm).

3.3. Antifungal applications

The antifungal applications of $MnAl_2O_4$nanoparticles were evaluated using the Agar Disc Diffusion Method against four different fungi: *Candida albicans*, *Candida tropicalis*, *A.niger*, and *M.piriformis*(Fig 5). Table-4 displays the measured zone of inhibition sizes, and the synthesized $MnAl_2O_4$nanoparticles exhibited effective antifungal activity against these selected fungi: *C.albicans*, *C.tropicalis, A.niger*and *M. piriformis,* respectively. All demonstrated inhibitory growth with good control of 3mm. As a result, $MnAl_2O_4$nano-particles had excellent antifungal properties.

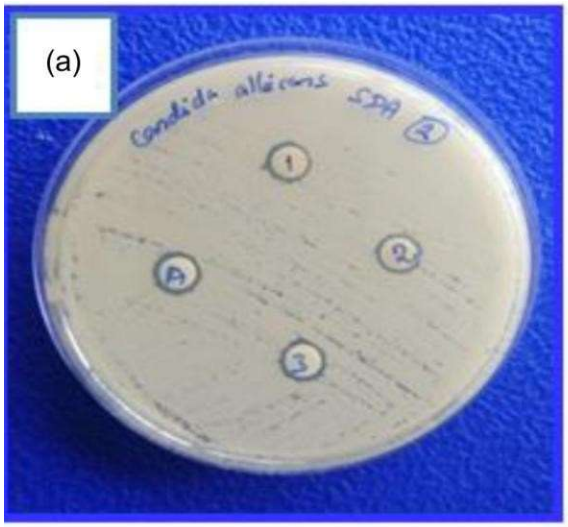

Candida albicans

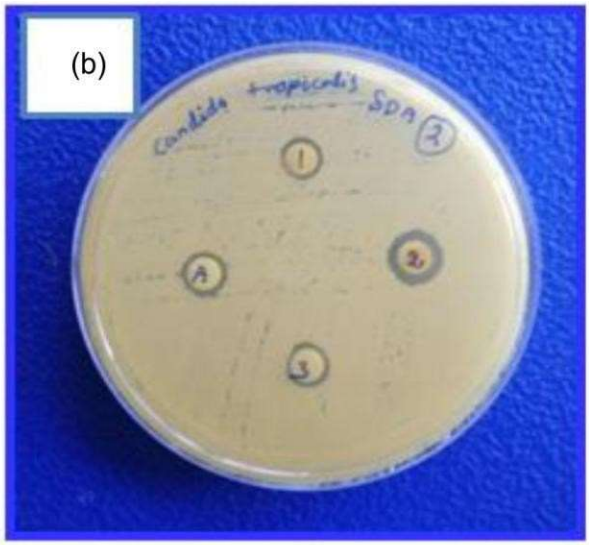

Candida tropicalis

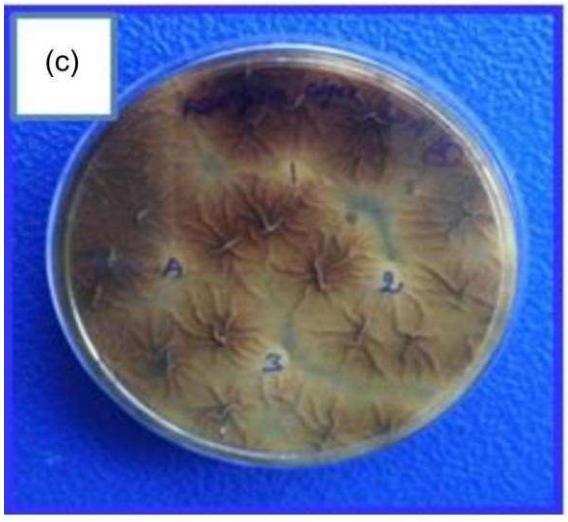

Aspergillus niger

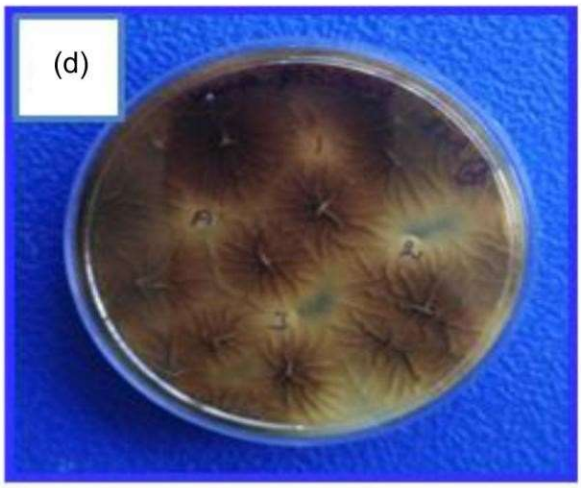

Mucor piriformis

Fig. 5. Antifungal application of $MnAl_2O_4$nanoparticles

Table-2: Inhibition zone of $MnAl_2O_4$nanoparticles against different fungi

Fungi	1000 (µg/mL)	Control
Candida albicans	3 mm	4 mm
Candida tropicalis	3 mm	4 mm
Aspergillusniger	3 mm	4 mm
Mucorpiriformis	3 mm	4 mm

4. CONCLUSIONS

A hydrothermal method was used to synthesize $MnAl_2O_4$nanoparticles. The phase study confirmed that $MnAl_2O_4$Nanoparticles were in the cubic phase. The synthesized compound exhibited a plate-like structure, according to the FE-SEM study. HRTEM results were consistent with the XRD results. The nanopowder synthesized in this study demonstrated excellent antibacterial activity towards *B.subtilis*and excellent antifungal performances towards the four selected fungal pathogens, and it was concluded that $MnAl_2O_4$nanoparticles had medical applications.

ACKNOWLEDGMENTS

The Department of Physics, Annamalai University and the "Centralized Instrumentation and Service Laboratory (CISL), Annamalai Nagar, India, are gratefully acknowledged by the researchers for providing instrumental facilities for their study.

CONFLICT OF INTEREST

The authors declare no conflict of interest.

REFERENCES

[1] F.Z. Akika, M.Benamira, H.Lahmar, M.Trari, I.Avramova, S.Suzer, *Surf. Interfaces,* 18, 100406 (2020).
[2] A.V. Belyaev, M.I. Lelet, N.I.Kirillova, N.M.Khamaletdinova, M.S.Boldin, A.A.Murashov, *Ceram Int.,* 45, 4835–4839(2019).
[3] P.Loiko, A.Belyaev, O.Dymshits, I.Evdokimov, V.Vitkin, K.Volkova, M. Tsenter, A.Volokitina, M.Baranov, E.Vilejshikova, *J. Alloys Compd*.,725, 998–1005 (2017).
[4] S.A.Mirbagheri, S.M.Masoudpanah, S.Alamolhoda, *Optik,* 204, 164170 (2020).
[5] S. Huang, Z.Wei, X.Wu, J.Shi, *J. Alloys Compd.,* 825, 154004 (2020).
[6] B.E.Azara, A.Ramazani, *Optik*, 208, 164129 (2020).
[7] G. Padmapriya and M. Sivachandiran, *Malaya J. Matematik*, S(2), 1081-1083(2020).
[8] T.Gholami, M.Salavati-Niasari, *Int. J. Hydrogen Energy*, 42, 17167-17177 (2017).
[9] M. Mosleh, *J. Mater. Sci. Mater. Electron*., 28, 773–777(2017).
[10] P. Bhavani, A. Manikandan, S.K.Jaganathan, S. Shankar and S.A. Antony, *J. Nanosci. Nanotechnol*., 18, 1388–1395 (2018).
[11] M.A.Subhana, P.C.Sahaa, A.Hossaina, Abdullah M. Asirib, M.M. Alam, *NanoscaleAdv*.,1-52(2021).
[12] J.Kong, J.Zhang, *Chem.Phys.Lett.,*806, 140053 (2022).
[13] G.Peng, S. Jiang, Y. Wang, Q. Zhang, *J. Cleaner Prod.*, 251, 119-725(2020).
[14] M. Huang, Y. Lin, H. Huang, X. Fan, *Electrochim.Acta*, 383, 138-353(2021).
[15] Z.Erda, Nurhayati, E.Amirudin,*J. Phys.: Conf. Series,* 2049, 012061 (2021).
[16] G. Mathubala, *Malaya J. Matematik*., Vol. S(2), 2243-2245 (2020).
[17] S. Wang, X. Wei, H.Gao, *Int. J. Light Electron Optics*., 185, 301–310(2019).
[18] X.Xu, R.G.ZinebSaghi, M. Gunter, *Nanotechnology*, 18, 225501 (2020).
[19] S.Wang, H.Gao, Y.Wei, Y.Li, X.Yang, L.Fang, L.Lei,*CrystEngComm*., 21, 263-277(2019) .
[20] A. Manikandan, M. Durka, S.A. Antony, *J.Inorg.Organomet.Polym. Mater.*,25, 1019–1031 (2018).
[21] T. Dhanasekaran, A. Padmanaban, K. Giribabu, R. Manigandan, S.P. Kumar, G. Gnanamoorthy, V. Narayanan, *Int. J. Eng. Sci*., 6, 57–59(2018).
[22] C.S. Rogerio-Navarro, R.R. de Avillez, *J. Mater. Res. Technol*.,9, 4194–4205 (2020).

[23] S.Gunalan, R.Sivaraj, V.Rajendran, *Progr. Nat.Sci.: Mater.Int.,* 22, 693-700 (2020).
[24] K.H.Jwad, T.H.Saleh, B.Abd-Alhamza,*Nano Biomed. Eng*., 11,3 (2019).
[25] S.A. Khan, S.Shahid, B.Shahid, *Biomolecules*,10, 785(2020).